

## Research Note

# Three globular cluster candidates in the direction of the bulge shown to be small emission nebulae<sup>\*</sup>

E. Bica<sup>1,\*\*</sup>, J.J. Clariá<sup>2,\*\*</sup>, Ch. Bonatto<sup>1</sup>, A.E. Piatti<sup>2,\*\*</sup>, S. Ortolani<sup>3,\*\*\*</sup>, and B. Barbay<sup>4</sup>

<sup>1</sup> Universidade Federal do Rio Grande do Sul, IF, Dept. de Astronomia, CP 15051, Porto Alegre 91501–970, RS, Brazil

<sup>2</sup> Observatorio Astronómico, Laprida 854, 5000 Córdoba, Argentina

<sup>3</sup> Università di Padova, Dept. di Astronomia, Vicolo dell'Osservatorio 5, I-35123 Padova, Italy

<sup>4</sup> Universidade de São Paulo, IAG, Dept. de Astronomia, CP 9638, São Paulo 01065–970, SP, Brazil

Received 27 February 1995 / Accepted 3 April 1995

**Abstract.** We carried out spectrophotometry in the range 4000–7000 Å and V, I and Gunn z imaging of the initially thought to be globular cluster candidates in the direction of the Galactic bulge TJ 5 and TJ 23 (Terzan & Ju 1980) and the one reported by Bica (1994). The three objects turned out to be small nebulae in rich stellar fields. Diagnostic diagrams for emission line ratios indicate that TJ 5 and TJ 23 are planetary nebulae. The locus of the third object strongly suggests it to be a supernova remnant, with very strong [NII]<sub>λ6584</sub> and strong [SII]<sub>λλ6717,31</sub>. The sizes of the nebulae are  $d=28''$ ,  $45''$  and  $49''$ , and the reddening derived from the Balmer decrement indicates  $E(B-V)=0.86$ ,  $1.81$  and  $0.19$ , respectively for TJ 5, TJ 23 and the supernova remnant.

**Key words:** ISM: planetary nebulae – ISM: supernova remnants – Galaxy: globular clusters: general – Galaxy: general

## 1. Introduction

The search and classification of reddened extended objects in the Galactic bulge direction, such as globular clusters, planetary nebulae (PN) and supernova remnants (SNR), are fundamental to derive their total populations and spatial distributions. Such studies have implications on a variety of subjects, from the distance to the Galactic centre and the chemical and dynamical evolutionary histories of the Galaxy, to the stellar evolution theory (see e.g. Racine & Harris 1989; Zinn 1985; Green 1991; Kaler 1985).

*Send offprint requests to:* E. Bica

<sup>\*</sup> Based on observations made at the Complejo Astronómico El Leoncito (CASLEO), Argentina, and European Southern Observatory (ESO), Chile.

<sup>\*\*</sup> Visiting astronomer at CASLEO.

<sup>\*\*\*</sup> Visiting astronomer at ESO.

Lists of globular clusters and globular cluster candidates (e.g. Webbink 1985; Racine & Harris 1989) included the objects TJ 5 ( $\alpha(1950) = 17^h 08' 08''$ ,  $\delta(1950) = -27^\circ 08' 0''$ ,  $l = 357.261^\circ$ ,  $b = 7.283^\circ$ ) and TJ 23 ( $\alpha(1950) = 17^h 41' 54''$ ,  $\delta(1950) = -32^\circ 45' 1''$ ,  $l = 356.686^\circ$ ,  $b = -1.916^\circ$ ) from Terzan & Ju (1980), who found them in a survey on R and I Schmidt plates. Bica (1994) found a diffuse object, hereafter referred to as B 1, on the ESO Sky Survey R Schmidt film #519 ( $\alpha(1950) = 17^h 21' 50''$ ,  $\delta(1950) = -24^\circ 15' 44''$ ,  $l = 1.411^\circ$ ,  $b = 6.393^\circ$ ), which resembled very reddened globular clusters in appearance. In order to clarify the exact nature of these objects and to derive their basic properties we provide in the present work detailed CCD spectrophotometry and imaging data, as part of a systematic study of non-stellar objects in the direction of the bulge, which we are carrying out. In Section 2 we present the observations, and in Sect. 3 we present the spectroscopic analysis. The concluding remarks are given in Sect. 4.

## 2. The observations

### 2.1. Spectroscopy

The spectroscopic observations were carried out with the 2.15m telescope at the Complejo Astronómico El Leoncito (CASLEO, San Juan, Argentina) on the night 9–10 June 1994. We employed the Universidade Federal do Rio Grande do Sul (UFRGS) CCD camera attached to the CASLEO Boller & Chivens Spectrograph. The detector is a GEC 6803 chip with  $578 \times 385$  pixels of size  $22 \times 22 \mu\text{m}$ ; one pixel corresponds to  $1.32''$  on the sky. The slit was oriented E–W. For TJ 5 and TJ 23 the slit was kept fixed whereas B 1 was scanned  $\approx 1'$  in the N–S direction due to its larger expected dimensions and because we were interested in its integrated properties as a possible globular cluster. Since the objects were not visible at the telescope monitor, the slit was

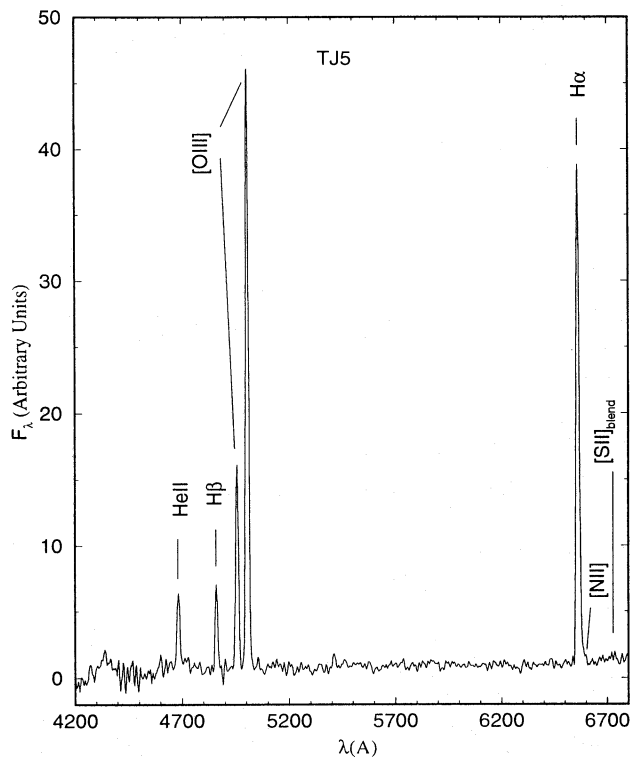


**Fig. 1a.** Wavelength and relative flux  $F_\lambda$  calibrated spectrum of the planetary nebula TJ 5

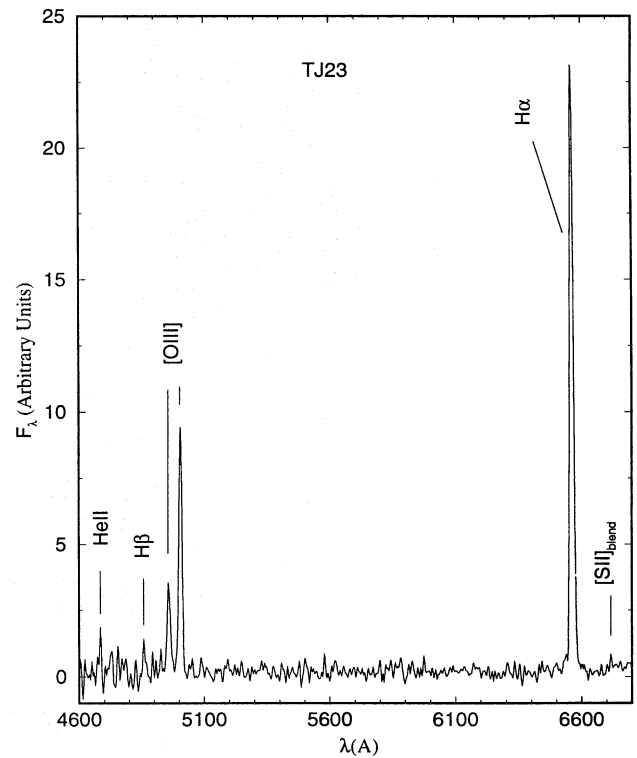


**Fig. 1b.** Same as 1a for the planetary nebula TJ 23

positioned by comparing stars in the field of view with the corresponding ones on the finding charts in Terzan & Ju (1980) and Bica (1994). We used a grating of 300 grooves  $\text{mm}^{-1}$  producing an average dispersion, in the observed region, of  $\approx 220 \text{ \AA mm}^{-1}$  or  $4.87 \text{ \AA pixel}^{-1}$ . A series of exposure times of 15 min each were employed for the objects giving a total of 60 min for TJ 23 and 75 min for TJ 5 and B 1. The long slit corresponding to  $3.3'$  on the sky allowed us to sample regions of background sky in spite of the crowded fields. The seeing during the night was typically  $\approx 2.5''$ . The slit width was  $4.5''$  resulting a resolution (FWHM) of  $\approx 14 \text{ \AA}$  as deduced from the He-Ne-Ar comparison lamp lines. Dome and sky flat fields were taken and employed in the reductions. The standard stars CD -32°9927 and LTT 377 (Stone & Baldwin 1993), and HD 160233 (Gutiérrez-Moreno et al. 1988), were observed for flux calibrations.

The reductions were carried out with the IRAF package following standard procedures using the SUN workstations at the Instituto de Física, UFRGS. The spectra were calibrated in relative  $F_\lambda$  units, since some clouds occurred during the night.

In Figs. 1a, 1b and 1c we show the resulting calibrated spectra, respectively for TJ 5, TJ 23 and B 1, in which we identify the emission lines. It is clear from the figures that we are dealing with emission nebulae.

## 2.2. Imaging

The broad-band images of TJ 5, TJ 23 and B 1 were obtained in May 1994 with the NTT 3.55m and the Danish 1.54m telescopes at the European Southern Observatory, La Silla, Chile.

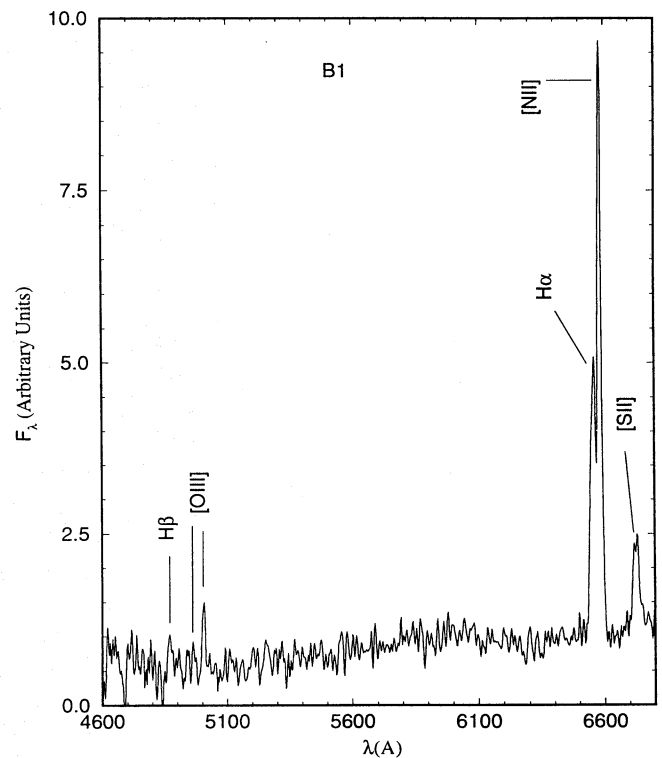


**Fig. 1c.** Same as 1a for the object B 1; notice the very strong  $[\text{NII}]_{\lambda 6584}$  line

The filters employed were Johnson's V (for B 1 only) and the

**Table 1.** Logbook of observations

B 1	May 15–16/NTT	May 17–18/Danish
Filter	Exp.Time (s)	Exp.Time (s)
V	60	600
I	4 × 60	60
z	60	600
TJ 5	May 15–16/NTT	May 17–18/Danish
I	60	60, 120
z	300	—
TJ 23	May 15–16/NTT	May 17–18/Danish
I	60	2 × 60
z	120	—

near-infrared Cousins' I and Gunn's z. The logbook of observations with exposure times is given in Table 1.

In the NTT observations the Nasmyth focus B was used equipped with a  $1024 \times 1024$  thinned Tektronix CCD (SUSI camera). The pixel size is  $24\mu\text{m}$ , corresponding to  $0.13''$  on the sky, with a total field of view of about  $2.2' \times 2.2'$ . At the Danish 1.54m telescope the CCD direct camera equipped with a Tektronix  $1024 \times 1024$  chip was used. The pixel size is again  $24\mu\text{m}$ , corresponding on the sky to  $0.37''$ . The total field of view is  $\approx 6.2' \times 6.2'$ . The images were reduced at the ESO computer center in Garching using the standard MIDAS procedure for bias subtraction, trimming, and flat-fielding.

As we were looking for reddened globular clusters we employed filters which were appropriate for these purposes. A careful analysis of the TJ 5 and TJ 23 images with IRAF on different intensity levels did not conclusively reveal the presence of the nebulae. Indeed, these objects are Planetary Nebulae (Sect. 3) and consequently the continuum is very weak, and in the bandpasses of the Cousins' I and Gunn's z filters, emission lines are as well very weak (*e.g.* in NGC 7027 the strongest line is  $[\text{ArIII}]_{\lambda 7751}$  with an intensity of  $\approx 3\%$  of that of  $\text{H}\alpha$ , Kaler et al. 1976).

Similarly, the emission nebula B 1 was not conclusively detected in the near-IR bandpasses nor in the V filter, since  $\text{H}\beta$  and the  $[\text{OIII}]$  lines are weak as compared to  $\text{H}\alpha$  (Fig. 1c). So far the nebula B 1 has been detected only on R band Schmidt plates because of the strong  $\text{H}\alpha$ ,  $[\text{NII}]_{\lambda 6584}$  and  $[\text{SII}]_{\lambda\lambda 6717,31}$  lines (Fig. 1c). Indeed, Tritton (1994, private communication) confirmed the presence of the extended object in a United Kingdom Schmidt Telescope plate in the R band, but not in an I plate, which suggested that it was an emission nebula instead of a globular cluster.

### 3. Discussion of the spectroscopy

#### 3.1. Emission line spectra

The emission lines in each spectrum were fitted with gaussians in order to obtain their fluxes. The reddening was estimated from

**Table 2.** Emission-line fluxes

	TJ 5		TJ 23		B 1	
	Obs.	Cor.	Obs.	Cor.	Obs.	Cor.
E(B–V)	0.0	0.86	0.0	1.81	0.0	0.19
$\text{HeII}_{\lambda 4686}$	103 $\pm 10$	117 $\pm 12$	95 $\pm 24$	127 $\pm 32$	—	—
$\text{H}\beta$	100 $\pm 10$	100 $\pm 10$	100 $\pm 20$	100 $\pm 20$	100 $\pm 20$	100 $\pm 20$
$[\text{OIII}]_{\lambda 4959}$	274 $\pm 14$	257 $\pm 13$	285 $\pm 28$	249 $\pm 25$	<46	<46
$[\text{OIII}]_{\lambda 5007}$	814 $\pm 41$	740 $\pm 37$	755 $\pm 75$	617 $\pm 62$	138 $\pm 28$	136 $\pm 27$
$[\text{NII}]_{\lambda 6548}$	11 $\pm 2$	4 $\pm 0.6$	<25	<4	415 $\pm 41$	340 $\pm 34$
$\text{H}\alpha$	722 $\pm 36$	287 $\pm 14$	2015 $\pm 101$	287 $\pm 14$	354 $\pm 35$	287 $\pm 29$
$[\text{NII}]_{\lambda 6583}$	33 $\pm 5$	13 $\pm 2$	<80	<11	1254 $\pm 125$	1020 $\pm 102$
$[\text{SII}]_{\lambda 6717}$	13 <sup>(1)</sup> $\pm 3$	5 <sup>(1)</sup> $\pm 1$	40 <sup>(1)</sup> $\pm 8$	5 <sup>(1)</sup> $\pm 1$	131 $\pm 13$	105 $\pm 10$
$[\text{SII}]_{\lambda 6731}$					146 $\pm 15$	117 $\pm 12$

**Table Notes.** (1) sum of fluxes of  $[\text{SII}]_{\lambda 6717}$  and  $[\text{SII}]_{\lambda 6732}$ ;  $[\text{NII}]_{\lambda 6548}$  and  $[\text{OIII}]_{\lambda 4959}$  have been constrained with the theoretical ratio 1:3 with respect to their stronger counterparts; uncertainties are given below each emission line flux.

the measured Balmer decrement assuming Case B of recombination ( $(\text{H}\alpha/\text{H}\beta)_0 = 2.87$ ) and a normal reddening law (Seaton 1979). The results are in Table 2 where the reddening corrected values are also listed, along with the E(B–V) used to deredden the fluxes.

We have used the diagnostic-diagram for the line-ratios  $\log(\text{H}\alpha/[\text{NII}]_{\lambda\lambda 6548,84}) \times \log(\text{H}\alpha/[\text{SII}]_{\lambda\lambda 6717,31})$  of Sabbadin & Bianchini (1977), following the loci indicated by Goudis et al. (1994) as based on enlarged samples, in order to characterize the spectra of our objects in terms of the physical conditions of the emitting gas. In this diagnostic-diagram (Fig. 2) the different loci correspond to SNRs, H II regions and PNe. TJ 5 and TJ 23 are clearly typical PN. The locus of B 1 is compatible with that of supernova remnants, with the  $[\text{NII}]$  lines somewhat stronger than those of a typical SNR. Notice that there is a class of PN with strong  $[\text{NII}]$  and  $[\text{SII}]$  (Fig. 2). However, B 1 is too far from that locus especially in terms of the ratio  $\text{H}\alpha/[\text{SII}]_{\lambda\lambda 6717,31}$ . Also in terms of  $\text{H}\beta/[\text{OIII}]_{\lambda\lambda 4959,5007}$ , B 1 has a value like that found in many SNR (Sabbadin & Bianchini 1977). This value denotes much less excitation than that observed in typical PN, thus reinforcing its identification as a SNR.

Also in terms of  $\text{H}\beta/[\text{OIII}]_{\lambda\lambda 4959,5007}$ , TJ 5 and TJ 23 are typical PN (Sabbadin & Bianchini 1977). Notice that in TJ 5 and TJ 23 the line  $\text{HeII}_{\lambda 4686}$  is slightly stronger than  $\text{H}\beta$  (Table 2), which indicates a high temperature for the central star.

In the dereddening procedure for B 1, we also tested an intrinsic ratio  $(\text{H}\alpha/\text{H}\beta)_0 = 3.0$ , which should be more appropri-

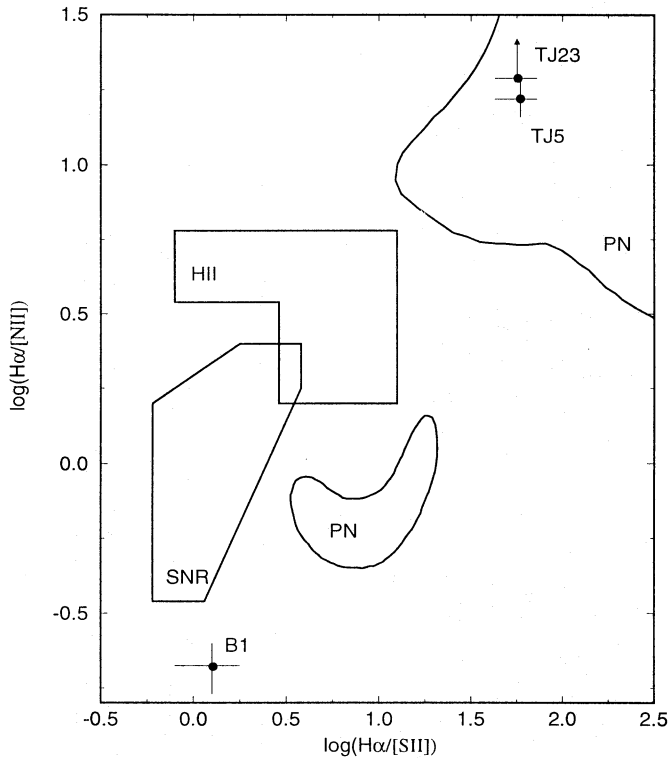


**Fig. 2.** Diagnostic-diagram for different classes of objects; notice that TJ 5 and TJ 23 are clearly typical planetary nebulae whereas B 1 lies close to the SNR locus. The arrow in TJ 23 indicates a lower limit for the line ratio

ate for SNR than that of Case B (2.87), since the former value is consistent with a large range of shock models (Shull & McKee 1979; Raymond 1979). However the latter assumption essentially does not change the locus of B 1 in Fig. 2. Consequently this uncertainty in the reddening corrections does not affect our conclusions.

Assuming that B 1 is a SNR and comparing our dereddened line-ratios (Table 2) with those of well-studied Galactic SNR (e.g. Leibowitz & Danziger 1983), we find that the  $H\beta/[OIII]_{\lambda\lambda 4959,5007}$  ratio resembles that of the middle-aged SNR IC 443. The  $H\alpha/[NII]_{\lambda\lambda 6548,84}$  ratio is lower than those in any SNR of that sample, the closest value being that of the young metal-rich SNR Cas A, whereas the  $H\alpha/[SII]_{\lambda\lambda 6717,31}$  ratio is similar to that observed in Vela, which has intermediate properties between young and middle-aged SNR (Raymond 1984). With respect to the young type I SNR Kepler, B 1 has a similar  $[SII]/H\alpha$  ratio but is less excited, as indicated by the stronger  $[NII]/H\alpha$  and weaker  $[OIII]/H\beta$  ratios.

### 3.2. Light profiles

We show in Figs. 3a, 3b and 3c light profiles perpendicular to the dispersion axis extracted from strong emission lines, respectively for TJ 5 and TJ 23 ( $H\alpha$ ), and B 1 ( $H\alpha + [NII]$ ). We also show the adjacent continuum extracted in a band  $\approx 200\text{\AA}$  wide blueward of  $H\alpha$ . The stellar fields are crowded, which explains why these extended objects have been suggested to be globular

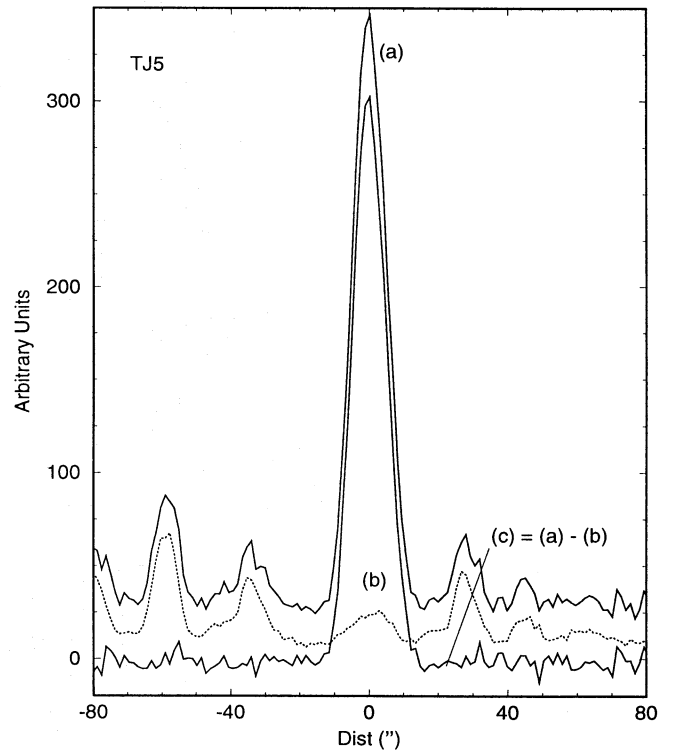


**Fig. 3a.** Light profiles for TJ 5 perpendicular to the dispersion axis for (a)  $H\alpha$ , (b) adjacent continuum and (c) subtraction (a)–(b); notice the continuum peak centred in the nebula which is probably the central star of this PN

cluster candidates, when seen through the R band in which gas emission is important. The subtraction of the continuum from the line profiles is also shown in Figs. 3a, 3b and 3c, so that the sizes of the emission nebulae can be more precisely measured in these star-free profiles. We derive angular diameters, at the base of the profiles, of  $d=28''$ ,  $45''$  and  $49''$  respectively for TJ 5, TJ 23 and B 1. The continuum profile of TJ 5 presents a conspicuous peak centred in the nebular emission (Fig. 3a), which might suggest that the central star of the PN has been detected in this case. Nevertheless we point out that there are several field stars superimposed on the nebula.

Since TJ 5 and TJ 23 are projected in the direction of the bulge we assumed an intrinsic size of planetary nebula  $D=0.11 \pm 0.04$  pc based on an average of 6 Galactic bulge PN from Dopita et al. (1990). We derived for TJ 5 a distance from the Sun of  $d_{\odot} = 0.80 \pm 0.28$  kpc, and for TJ 23,  $d_{\odot} = 0.50 \pm 0.17$  kpc. Rather, these relatively short distances may suggest that the objects are disk PN. The colour excesses obtained from the  $H\alpha/H\beta$  ratio (Sect. 3.1) imply  $A_V = 2.67$  and  $5.61$ , respectively for TJ 5 and TJ 23 (adopting  $A_V/E(B-V)=3.1$ ). These values indicate an absorption of  $\approx 3.3 \text{ mag kpc}^{-1}$  in the direction of TJ 5 and  $\approx 11.2 \text{ mag kpc}^{-1}$  in that of TJ 23. The very high value for TJ 23, can be explained by its lower Galactic latitude (Sect. 1) and the large concentration of dust clouds in directions close to the Galactic centre. In the case of TJ 5, at  $b = 7.283^\circ$ , intervening nearby dust clouds are evident in the Sky Survey Schmidt plates.

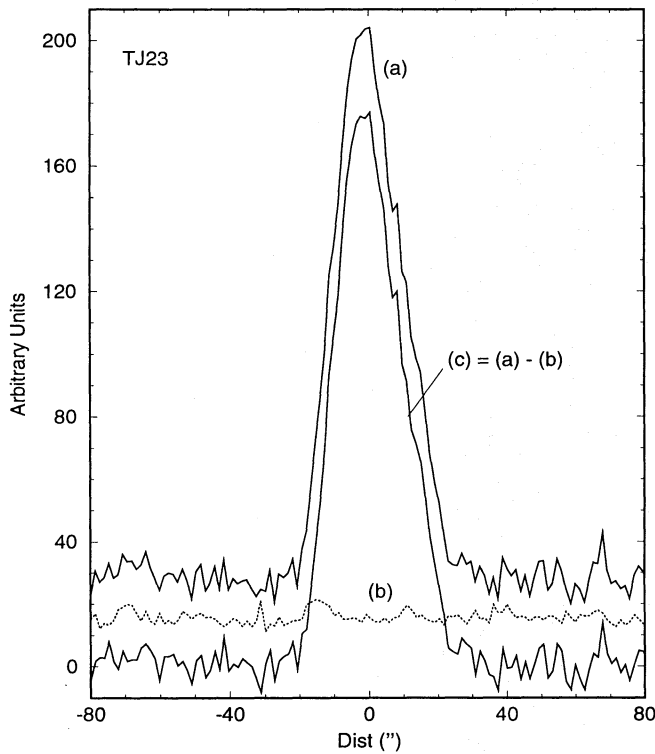


Fig. 3b. Same as 3a for TJ 23

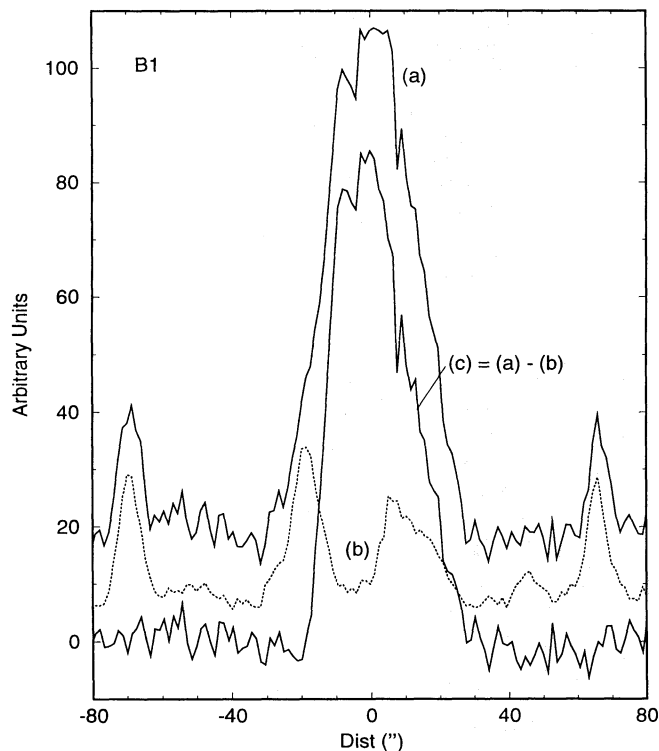


Fig. 3c. Same as 3a for B 1; in this case the emission line profile includes  $H\alpha + [NII]$

Based on the spectral similarities of B 1 with respect to well-known SNRs as discussed in Sect. 3.1, we can use their intrinsic

sizes to estimate the distance. Taking the size of the young SNR Cas A,  $D \approx 3$  pc (Milne 1970) as reference for B 1, we derive a distance of  $d_{\odot} = 12.6$  kpc; on the other hand, assuming the typical larger size of middle-aged SNR ( $D \approx 18$  pc) the resulting distance would put B 1 outside the Galaxy. This suggests that if indeed B 1 is a SNR it should be young. The Galactic latitude (Sect. 1) and the distance from the Sun  $d_{\odot} = 12.6$  kpc would place B 1 at  $z \approx 1.4$  kpc above the Galactic plane, a value comparable to that of the type I SNR Kepler.

#### 4. Concluding remarks

The emission lines in our spectral observations clearly show that the previous globular cluster candidates TJ 5, TJ 23 and B 1 are in fact small emission nebulae; the angular sizes of the nebulae are respectively  $d=28''$ ,  $45''$  and  $49''$ . The objects are reddened, as deduced from the  $H\alpha/H\beta$  emission line ratio, with  $E(B-V)=0.86$ ,  $1.81$  and  $0.19$  respectively for TJ 5, TJ 23 and B 1. Diagnostic diagrams indicate that TJ 5 and TJ 23 are typical planetary nebulae, whereas B 1, with strong  $[NII]_{\lambda 6584}$  and  $[SII]_{\lambda\lambda 6717,31}$ , is located in the region of SNRs. Some planetary nebula spectra are known to present enhanced  $[NII]_{\lambda 6584}$  and  $[SII]_{\lambda\lambda 6717,31}$ , however, the latter lines do not overlap the SNR locus. Assuming as typical size of PND  $= 0.11 \pm 0.04$  pc, we find distances to TJ 5 and TJ 23 of, respectively,  $d_{\odot} = 0.80 \pm 0.28$  kpc and  $d_{\odot} = 0.50 \pm 0.17$  kpc. Adopting an intrinsic size like those of typical young SNRs, we estimate for B 1 a distance of  $d_{\odot} = 12.6$  kpc and  $z \approx 1.4$  kpc above the Galactic plane.

If B 1 is confirmed as a SNR it would add to the small sample of optically identified ones in the Galaxy. Only a small fraction of the known SNRs can be optically observed because of strong dust absorption close to the Galactic plane; van den Bergh (1978) detected 29 of them. B 1 is not listed in any SNR catalogue based on Radio, infrared and X-rays observations. It may have been missed in Radio surveys because of its small angular size, since only recently surveys with resolution of  $\approx 1'$  are becoming available (Green 1984). B 1 is not present in the list of 157 Galactic SNR which were detected or have upper limits in the IRAS data (Arendt 1989). It is also absent in the X-ray catalogue of 47 Galactic SNR compiled by Seward (1990) with *Einstein* observations.

Narrow-band filter images in the lines  $H\alpha$ ,  $[NII]_{\lambda 6584}$  and  $[SII]_{\lambda\lambda 6717,31}$ , together with high spatial resolution observations in X-Ray and Radio would be fundamental to study in detail the structure of B 1. Also, the determination of the velocity field would help to definitely establish (or not) its nature as a SNR.

**Acknowledgements.** JJC, AEP and EB thank the staff at CASLEO, and SO that at ESO, for hospitality and assistance during the observations. EB thanks Dr. Susan Tritton for the kind letter of June 14, 1994 communicating her conclusions from the analysis of R and I UKST plates. This work was partially supported by the Brazilian institutions CNPq and FINEP, as well as CONICOR and CONICET from Argentina.



## References

- Arendt, R.G. 1989, ApJS, 70, 181  
Bica, E. 1994, A&A, 285, 868  
Dopita, M.A., Henry, J.P., Tuohy, I.R. et al., 1990, ApJ., 365, 640  
Goudis, C.D., Christopoulou, P.-E., Meaburn, J. & Dyson, J.E. 1994, A&A, 285, 631  
Green, D.A. 1984, MNRAS, 209, 449  
Green, D.A. 1991, PASP, 103, 209  
Gutiérrez-Moreno, A., Moreno, H., Cortés, G. & Wenderoth, E. 1988, PASP, 100, 973  
Kaler, J.B., Aller, L.H., Czyzak, S.J. & Epps, H.W. 1976, ApJS, 31, 163  
Kaler, J.B. 1985, ARA&A, 23, 89  
Leibowitz, E.M. & Danziger, I.J. 1983, MNRAS, 204, 273  
Milne, D.K. 1970, Aust. J. Phys, 23, 425  
Racine, R. & Harris, W.E. 1989, AJ, 98, 1609  
Raymond, J.C. 1979, ApJS, 39, 1  
Raymond, J.C. 1984, ARA&A, 22, 75  
Sabbadin, F. & Bianchini, A. 1977, A&A, 55, 177  
Seaton, M.J. 1979, MNRAS, 187, 73p  
Seward, F.D. 1990, ApJS, 73, 781  
Shull, J.M. & McKee, C.F. 1979, ApJ, 227, 131  
Stone, R.P.S. & Baldwin, J.A. 1983, MNRAS, 204, 347  
Terzan, A. & Ju, K.H. 1980, ESO Messenger #20, 6  
van den Bergh, S. 1978, ApJS, 38, 119  
Webbink, R.F. 1985, in "Dynamics of star clusters", IAU Symp. 113, ed. J. Goodman and P. Hut (Reidel, Dordrecht), p.541  
Zinn, R. 1985, ApJ, 293, 424

This article was processed by the author using Springer-Verlag  $\mathrm{T}_{\mathrm{E}}\mathrm{X}$  A&A macro package 1992.